Investigation of the energetic and exergetic performance of hybrid rotary desiccant-vapor compression cooling systems using different refrigerants

Çerçi, K.N.; Oliveira Silva, I.S.; Hooman, K.

DOI
10.1016/j.energy.2024.131732

Publication date
2024

Document Version
Final published version

Published in
Energy

Citation (APA)
Çerçi, K. N., Oliveira Silva, I. S., & Hooman, K. (2024). Investigation of the energetic and exergetic performance of hybrid rotary desiccant-vapor compression cooling systems using different refrigerants. *Energy*, *302*, Article 131732. https://doi.org/10.1016/j.energy.2024.131732

Energy 302 (2024) 131732

Contents lists available at ScienceDirect

Energy

journal homepage: www.elsevier.com/locate/energy

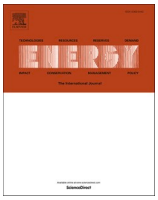

Investigation of the energetic and exergetic performance of hybrid rotary desiccant-vapor compression cooling systems using different refrigerants

Kamil Neyfel Çerçi [a,b,*], Ivo Rafael Oliveira Silva [a,c], Kamel Hooman [a]

[a] Department of Process and Energy, Delft University of Technology, Leeghwaterstraat 39, 2628CB, Delft, the Netherlands
[b] Tarsus University, Faculty of Engineering, Department of Mechanical Engineering, 33400, Tarsus, Mersin, Turkiye
[c] University of Coimbra, Faculty of Science and Technology, Department of Mechanical Engineering, 3030-788, Coimbra, Portugal

ARTICLE INFO

Handling editor: Wojciech Stanek

Keywords:
Desiccant wheel
Vapor compression
Hybrid cooling
Refrigerants
Energy
Exergy

ABSTRACT

In this study, a desiccant-based hybrid cooling system supported by a vapor compression system and a heat recovery unit (rotary heat wheel) was analyzed from energetic and exergetic perspectives during the daily working hours of an office building in Istanbul to meet the desired comfort conditions. We focus on the impact of different refrigerants; namely R32, R1234yf, R290, R134a, R600a, R245fa, and R717, on hybrid rotary desiccant-vapor compression systems. While the highest electricity consumption was obtained in the system using R1234yf, the lowest electricity consumption was achieved with R717. However, with the effectiveness of the desiccant wheel, the best results were obtained for R1234yf with those pertinent to R717 at the other extreme. Considering the total electricity consumption of the system, the highest energetic and exergetic performance parameters were achieved with the use of R717 as the refrigerant. Compared to R1234yf, the daily average energetic performance parameters obtained with R717 increased by 22.3 % for COP_r, 21.8 % for COP_{el}, and 4.7 % for COP_{th}. Similarly, compared to R1234yf, the daily average exergetic performance parameters in R717 presented increases of 13.6 % for $COP_{x,el}$, 7.5 % for $COP_{x,th}$, and 8.1 % for η_x.

1. Introduction

Burning fossil fuels leads to emission of greenhouse gases (GHG) which, in turn, hinder return of heat radiation from the Earth's surface to space and contributes to global warming [1]. There is a strong correlation between economic growth, energy consumption and emissions of carbon dioxide. The building sector accounts for about 40 % of the total energy consumption worldwide, to which the increasing demand for thermal comfort, predominantly met by the use of vapor compression systems, is a major contributor [2].

In typical vapor compression systems (VC), the process air is cooled below the dewpoint to reduce the humidity content and then heated to meet the required indoor conditions; for instance as recommended by ASHRAE. In humid regions the latent load, to lower the humidity level to meet the comfort requirement, is high therefore the evaporator temperature is lowered leading to an increase in the compressor energy consumption and, consequently, the system coefficient of performance (COP) is reduced [3]. The latent load can be handled, separately from the sensible load, using desiccants with hygroscopic properties that adsorb (solid) or absorb (liquid) the excessive moisture present in the air. Hence, solid desiccant cooling systems, utilizing a rotary desiccant wheel to extract moisture from air, offer an attractive solution. In such systems, the rotary desiccant wheel adsorbs water vapor due to the vapor pressure difference between its surface and the surrounding air. To ensure continuous operation of the system, the adsorbed water vapor needs to be removed from the desiccant wheel. Regeneration heat is applied to the desiccant wheel for this process. The air leaving the wheel will be dry and warm therefore it needs to be treated for achieving the desired indoor comfort conditions. Such rotary desiccant cooling systems can be combined with solar collectors and evaporative coolers to minimize the overall energy consumption required for building air-conditioning. In this way, these systems form hybrid rotary desiccant cooling systems [4–6]. Many researchers have investigated hybrid rotary desiccant cooling systems to reduce energy consumption and make the system more appealing. T.S. Ge et al. [7] compared the performance of a solar driven rotary desiccant cooling system with that of a conventional vapor compression system in two different climates. The solar driven desiccant cooling system was able to meet the load requirement

* Corresponding author. Department of Process and Energy, Delft University of Technology, Leeghwaterstraat 39, 2628CB, Delft, the Netherlands.
E-mail addresses: kneyfelcerci@tarsus.edu.tr, K.N.C.Cerci@tudelft.nl (K.N. Çerçi).

https://doi.org/10.1016/j.energy.2024.131732
Received 15 January 2024; Received in revised form 8 April 2024; Accepted 20 May 2024
Available online 24 May 2024

Nomenclature	
A	area (m)
c	regression coefficient
c_p	specific heat (kJ/kg)
$\dot{m}$	mass flow rate (kg/h)
N	the rotation speed of the wheel (rev/h)
$\dot{E}$	energy rate (kW)
h	specific enthalpy (kJ/kg)
ΔP	pressure drop (kPa)
s	specific entropy (kJ/kg)
ΔT	temperature difference (°C or K)
V	air frontal velocity (m/s)
$\dot{V}$	volumetric flow rate (m^3/s)
$\dot{X}$	exergy rate (kW)
Greek symbols	
ε	effectiveness (−)
ψ	specific flow exergy (J/kg)
ω	humidity ratio (kg_w/kg_{da})
η	efficiency (dec or %)
λ_{l-v}	latent heat of evaporation (kJ/kg)
Subscripts	
0	dead state
amb	ambient
p,a	process air
r,a	regeneration air
DW	desiccant wheel
d	destruction
RHX	rotary heat exchanger
r	refrigerant
sc	subcooling
sh	superheating
is	isentropic
mec	mechanic
e	evaporator
cnd	condenser
cmp	compressor
cmp,el	electricity consumed by compressor
csm	total electricity consumed by system
ev	expansion valve
s	sensible
l	latent
t	Total
th	thermal
el	electrical
RAH	Regeneration air heater
reg	Regeneration
d,t	total destruction
i,set	indoor air set point
c,t	total cooling
Abbreviations	
COP	coefficient of performance
EU	European Union
GWP	global warming potential
ODP	ozone depleting potential
VCS	vapor compression system
DW-VC	hybrid rotary desiccant- vapor compression
DW	desiccant wheel
RHX	rotary heat exchanger

in both cities and showed a reduction in electricity consumption. However, it presents a higher initial investment cost. Olmuş et al. [8] simulated a rotary desiccant-based air conditioning system integrated with direct evaporative cooler, dew point indirect evaporative cooler, and heat recovery units throughout a complete cooling season for an office building located in Adana, Turkey. The thermal and electrical energy requirements of the system are provided by Photovoltaic/Thermal (PV/T) units. The seasonal thermal, electrical, and overall performance coefficients of the system are obtained as 0.46, 4.09, and 0.42, respectively. Çalışkan et al. [9] evaluated a desiccant air cooling system incorporating a desiccant wheel, sensible heat wheel, and regenerative evaporative cooler energetically and exergetically. The researchers emphasized that improvements to the system should be made in the order of the desiccant wheel, regenerative evaporative cooler, and sensible heat wheel.

Another type of hybrid rotary desiccant cooling systems is the hybrid rotary desiccant-vapor compression cooling systems (DW-VC). In these systems, the hot and dry air exiting the desiccant wheel is provided by the evaporator used for post-cooling, while the thermal energy recovered from the condenser can regenerate the desiccant wheel. Thus, hybrid DW-VC cooling systems offer significant energy savings potential. Another advantage of these systems is their compact structure [10,11]. For this reason, many researchers have conducted studies on DW-VC cooling systems [6,10,12,13]. Ge et al. [14] investigated the saving potentials of a desiccant assisted hybrid air source heat pump with four running modes (heating, cooling, dehumidification, cooling and dehumidification) in China. The hybrid system has generally less energy consumption compared with the conventional system in terms of

primary energy consumption for all processes. In terms of energy consumption, the system parameters have improved, but R22 was used as a refrigerant in that study. Due to the ozone-depleting effect of R22 and its contribution to global warming, its use has been banned in many places as of 2020. Liu et al. [15] compared the energy consumption of a vapor compression refrigeration system and a solid-desiccant hybrid system. They considered the use of different fuels to achieve the desired regeneration temperature. The results show that coupling the conventional system with a rotary desiccant wheel provides energy savings on using natural gas or solar energy. But the researchers used heaters to provide the heat of regeneration. R22 refrigerant, which is prohibited to be used today, was used as a refrigerant in the system. Hürdoğan et al. [16] conducted an exergy analysis of the desiccant cooling system based on different dead-state conditions. In this system, the process air exiting the desiccant wheel and heat exchangers provided indoor temperature conditions through the cooling unit running on R134a. In order to evaluate the individual performance of each component in the system, exergy equations for all components were presented. Within the dead-state temperature range of 0–30 °C, the exergetic efficiency for the entire system ranged between 32 % and 10 %. Jani et al. [17,18] investigated the different performance parameters of a hybrid solid desiccant-vapor compression system in a hot and humid climate. The required regeneration heat in the system was provided by the electric heater. Those researchers emphasized that hybrid solid desiccant cooling systems improve performance parameters, are environmentally friendly, and have the capacity to enhance indoor air quality. No information was provided about the working fluid used in the VCR. Tu et al. [19] investigated, in terms of energy and exergy aspects, 6 different desiccant cooling systems to analyze the effect of irreversible processes on the performance of these systems. The results illustrated that exergy destruction can be reduced by replacing the direct evaporative cooler with a sensible heat exchanger and an electric heater with a heat pump. The effects of different types of refrigerants were not considered. Sheng et al. [20] conducted several experimental studies to observe energy performance parameters in high temperature heat pump desiccant wheel systems. It was found that the regeneration temperature, outdoor humidity ratio, and the ratio of regeneration to process air flow rate significantly affect the dehumidification capacity of the desiccant wheel. The COP of the conventional desiccant wheel coupled with a high-temperature heat pump reached a maximum value of 2.08 using BY-3 as the refrigerant. Sheng et al. [21] investigated coupled high-temperature heat pump using R134a - rotary dehumidification systems using R134a in two different configurations from both an energetic and exergetic perspective. The results demonstrated that the high-temperature heat pump integrated with the desiccant wheel system eliminates significant exergy destruction caused by the electric heater. The researchers achieved a 46.9 % increase in exergetic efficiency, while energy efficiency improved by 19 %. Basso et al. [22] integrated a transcritical CO_2 heat pump into a desiccant air conditioning system to reduce the contribution of external thermal sources and examined the variations in the system's energy performance parameters. While the system's regeneration heat is provided through solar collectors, the electrical demand of the transcritical CO_2 heat pump is met by PV panels. The COP_{th} values for the hybrid system were obtained as 0.36 for Milan, 0.61 for Rome and Palermo, and COP_{el} values were 0.9 for Milan, 1.75 for Rome, and 1.78 for Palermo. Tian et al. [11] examined a combined heat pump rotary desiccant cooling system for nearly zero-energy buildings to address high humidity issues. They analyzed the system energetically under different scenarios and compared it to a traditional air conditioning system. The type of refrigerant was not mentioned in this study. The results indicated an overall performance improvement in indoor environmental control and energy savings compared to traditional air conditioning systems. Additionally, the optimal pre-cooling evaporator outlet temperature was found to be 14 °C.

In the literature, numerous studies have been conducted to enhance the performance, reduce the size and cost of hybrid DW-VC cooling systems, aiming to increase competitiveness in the market and contribute to the goals of nearly zero-energy buildings [11]. A limited portion of these studies discussed the type of refrigerant used as working fluid (namely R22, R134a, R410a, and BY-3). Since these studies employ a single refrigerant in hybrid DW-VC cooling systems, the extent to which the refrigerant enhances the system cannot be fully understood. Therefore, in the existing literature, neither theoretical nor experimental studies have been encountered regarding the impact of different refrigerants on hybrid DW-VC cooling systems. This study addresses the effects of various refrigerants on the hybrid DW-VC cooling system from energetic and exergetic perspectives. The refrigerants used in the simulation are R32, R1234yf, R290, R134a, R600a, R245fa, and R717. The use of most of these refrigerants utilized in the simulation has not been found in the literature for hybrid DW-VC cooling systems. This makes the results obtained from the study even more intriguing. R290

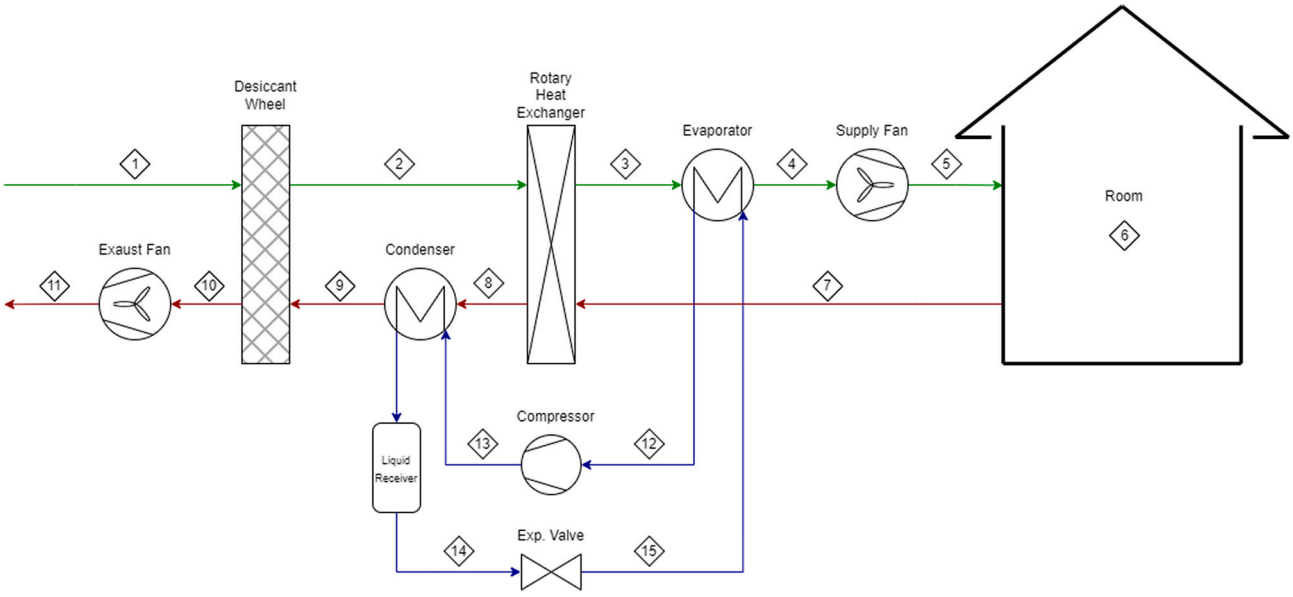

Fig. 1. Schematic view of the hybrid cooling system.

Table 1
The main input data for cooling load calculations.

Parameter	Value	Units
Roof U-Value	0.48	W/m^2K
Ground U-Value	0.30	W/m^2K
External Wall U-Value	0.32	W/m^2K
Windows U-Value	2.7	W/m^2K
Doors U-Value	0.070	W/m^2K
Occupancy	18.6	m^2/person

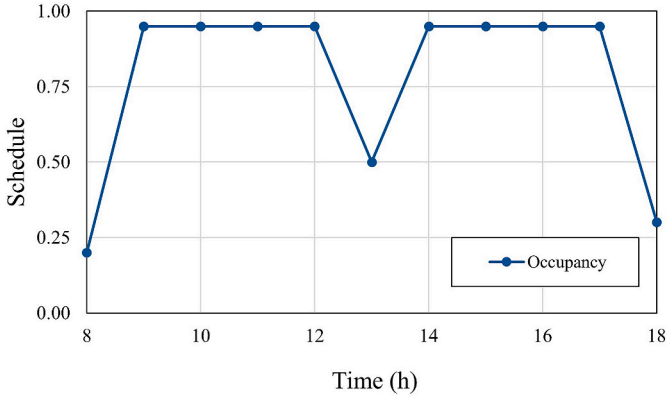

Fig. 2. Schedule profiles of the occupancy loads during office working hours.

and R600a are hydrofluorocarbons (HFCs), whereas R717 is a natural refrigerants fluid. The common feature of these three refrigerants is that they have very low Global Warming Potential (GWP) values. R1234yf is a synthetic refrigerant with a similarly low GWP value. R32, R134a, and R245fa have high GWPs, leading to their restricted use by EU Regulation 517/2014 [23]. The reason for using these refrigerants in the analyses is to compare their effects on the system with those of low Global Warming Potential (GWP) refrigerants. We believe that the results presented in this study will raise awareness and serve as inspiration for many researchers and manufacturers.

2. System description

A schematic diagram of the proposed system is shown in Fig. 1. The system combines a desiccant wheel, a rotary heat exchanger, a vapor compressor unit and two fans.

On the process side (from 1 to 5), outside ambient air flows through the desiccant wheel (1 → 2). Here, the humidity in the air is reduced and the air temperature increases due to heat and mass transfer in the

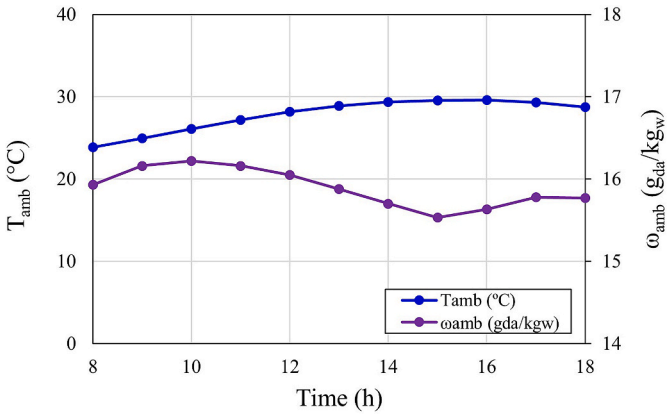

Fig. 3. Variations in temperature and absolute humidity during office working hours for the day (August 23rd) with the highest cooling load in July.

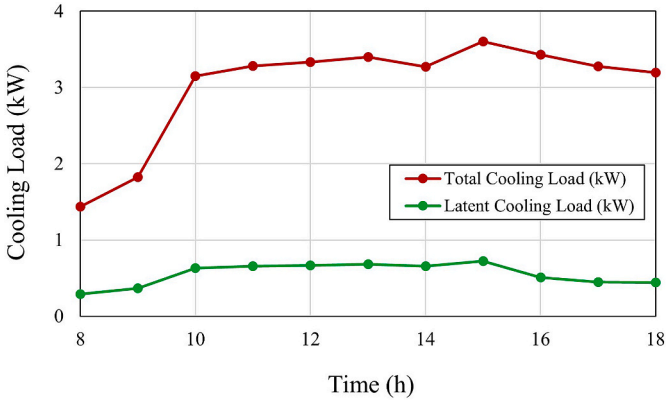

Fig. 4. Variations in total and latent cooling loads during office working hours.

desiccant wheel matrix. To reduce the load on the evaporator, the hot and dry air is first sensibly cooled in the rotary heat exchanger (2 → 3) and then cooled to the desired supply air temperature in the evaporator (3 → 4).

On the regeneration side (from 7 to 11), the cool air extracted from the room is blown into the rotary heat exchanger (7 → 8). The sensible energy exchange with the process side raises the air temperature. To reduce energy consumption from possible external sources, the heat dissipated from the condenser is used to raise the air temperature to the regeneration temperature (8 → 9). The regeneration process (9 → 10) removes excess moisture from the desiccant material to allow continuous operation of the system.

In a vapor compression refrigeration unit (from 12 to 15), the working fluid evaporates in the evaporator, which absorbs heat from the process air, and then enters the compressor (15 → 12). The working fluid, with increased pressure and temperature in the compressor (12 → 13), condenses in the condenser by releasing heat to the regeneration air (13 → 14). Subsequently, through the expansion valve, the pressure and temperature of the working fluid are reduced, allowing it to reach the evaporator state again (14 → 15).

3. Building and cooling load procedures

To fully evaluate the performance of the desiccant cooling hybrid system a 100 m^2 office situated in Istanbul was selected. According to the Koppen classification, Istanbul is a good candidate due to the humid subtropical climate with no dry months in summer. The climate data for Istanbul was gathered using the TRNSYS software (Meteonorm data) [24]. The building construction materials and design loads were selected according to Turkish Standard 825 [25] and ASHRAE 90.1 [26], respectively. Table 1 summarizes the main input data for cooling load calculations. The cooling loads were obtained using the EnergyPlus software [27]. Fig. 2 shows the schedule profiles of the occupancy loads in a typical office workday (from 8:00 to 18:00). The ambient outdoor conditions and the cooling loads for the worst cooling day are presented in Figs. 3 and 4. During office working hours, the temperature and absolute humidity values varied between 23.86 - 29.6 °C and 15.53–16.22 g_w/kg_{da}, respectively. The total cooling load fluctuated between 1.44 and 3.61 kW throughout the day. The cooling load reached its peak value at 15:00.

4. Modelling of components

4.1. Desiccant wheel model (DW)

In this study, the building latent cooling load was removed using a desiccant wheel (DW). It was assumed that the DW operated in the balanced flow, and the process and regeneration airflow rates were

taken to be the same ($A_{pa}/A_{ra} = 1$ and $\dot{m}_{pa} = \dot{m}_{ra}$). The dimensions of the desiccant wheel were assumed to be 440 mm × 200 mm, and silica gel was used as the desiccant material. Throughout the study, the rotation speed of the desiccant wheel (N_{DW}) was assumed to be 12 rev/h. Multiple Linear Regression (MLR) models, as suggested in the literature, were used to calculate the outlet conditions of the process air for the DW. The experimental validation of the existing DW model was conducted in the relevant study [28], and it was indicated that the model could be used with confidence by researchers.

$$\widehat{Y} = c_0 + \sum_{i=1}^{m} c_i x_i + \sum_{i=1}^{m} \sum_{\substack{j=1 \\ (j \geq i)}}^{m} c_{ij} x_i x_j \tag{1}$$

where $\widehat{Y}$ is $\widehat{T}_2$ or $\widehat{\omega}_2$, x is independent variable (T_1, ω_1, T_9, ω_9, N_{DW}, V_{DW}), m is the number of input variables and c is the coefficient. The coefficients for temperature and absolute humidity in this MLR equation are presented in Table A.1 in **Appendix A**.

The properties of the air exiting the regeneration channel of the desiccant wheel (DW) were calculated using mass and energy balance. In this context, heat loss from the DW was disregarded [29].

$$\dot{m}_{p,a}(\omega_2 - \omega_1) = \dot{m}_{r,a}(\omega_9 - \omega_{10}) \tag{2}$$

$$\dot{m}_{p,a}(h_2 - h_1) = \dot{m}_{r,a}(h_9 - h_{10}) \tag{3}$$

The dehumidification effectiveness of the desiccant wheel (ε_{DW}) is expressed by Eq. (4) [29]:

$$\varepsilon_{DW} = \frac{\omega_1 - \omega_2}{\omega_1} \tag{4}$$

To calculate the exergy destruction ($\dot{X}_d$), it is necessary to determine the flow exergy (ψ) at the inlet and outlet conditions of each equipment. Eq. (5) provided the general flow exergy (ψ) expression [30].

$$\psi = (h - h_0) - T_0(s - s_0) \tag{5}$$

where, state 0 represents the dead state, and state 1 denotes the external ambient state in the system. In the study, the dead state is assumed to be the same as the external ambient state.

The following equation can be utilized for the exergy analyses of the DW [9,31].

$$\dot{X}_{DW} = \dot{m}_{p,a}(\psi_1 - \psi_2) + \dot{m}_{r,a}(\psi_9 - \psi_{10}) \tag{6}$$

4.2. Rotary heat exchanger model (RHX)

To enhance the system performance, a Rotating Heat Exchanger (RHX) was employed between the process and regeneration air channels. The dimensions of the RHX are assumed to be the same as those of the DW. The effectiveness method was utilized in the operation of the RHX [32].

$$\dot{E}_{max,RHX} = C_{min,RHX}\left(T_{cold,RHX} - T_{hot,RHX}\right) \tag{7}$$

$$\dot{E}_{RHX} = \varepsilon_{RHX}\dot{E}_{max,RHX} \tag{8}$$

$$\dot{E}_{RHX} = \dot{m}_{p,a}(h_2 - h_3) \tag{9}$$

$$\dot{E}_{RHX} = \dot{m}_{r,a}(h_8 - h_7) \tag{10}$$

where, $C_{min,RHX} = \dot{m}c_p$ represents the minimum capacitance rate (C) between the hot and cold fluids. ε_{RHX} is the effectiveness of the rotating heat exchanger and is assumed to be 0.85 [33].

The following equation were used for the exergy calculations of the RHX [31].

$$\dot{X}_{RHX} = \dot{m}_{p,a}(\psi_2 - \psi_3) + \dot{m}_{r,a}(\psi_7 - \psi_8) \tag{11}$$

4.3. Vapor compression system model (VCS)

A traditional vapor compression unit, composed of evaporator, condenser, expansion valve, and compressor, was used to meet the regeneration heat and post-cooling of DW. The following assumptions, commonly used in the literature for vapor compression systems [34,35], were employed.

- ✓ A temperature difference of 10 °C is assumed between the evaporation temperature and the air leaving the evaporator to cool the process air.
- ✓ A temperature difference of 10 °C is assumed between the condensation temperature and the air leaving the condenser for the regeneration heat.
- ✓ The throttling process at the expansion valve is considered isenthalpic.
- ✓The isentropic and mechanical efficiencies of the compressor are assumed to be 0.8 and 0.95, respectively.
- ✓ Temperature differences of 3 K are accepted for superheating and subcooling.

Based on the above assumptions, the following equations were used for the energy and exergy analyses of the evaporator [30,36].

$$\dot{E}_{e,s} = \dot{m}_{p,a}c_{p_{p,a}}(T_3 - T_4) \tag{12}$$

$$\dot{E}_{e,l} = \dot{m}_{p,a}\lambda_{l-v}(\omega_3 - \omega_4) \tag{13}$$

$$\dot{E}_e = \dot{E}_{e,s} + \dot{E}_{e,l} \tag{14}$$

$$\dot{E}_e = \dot{m}_r(h_{12} - h_{15}) \tag{15}$$

$$\dot{X}_e = \dot{m}_r(\psi_{15} - \psi_{12}) + \dot{m}_{p,a}(\psi_3 - \psi_4) \tag{16}$$

The following equations were used for the energy and exergy analyses of the condenser [30].

$$\dot{E}_{cnd} = \dot{m}_{p,a}(h_9 - h_8) \tag{17}$$

$$\dot{E}_{cnd} = \dot{m}_r(h_{13} - h_{14}) \tag{18}$$

$$\dot{X}_{cnd} = \dot{m}_r(\psi_{13} - \psi_{14}) + \dot{m}_{p,a}(\psi_8 - \psi_9) \tag{19}$$

The following equations can be utilized for the energy and exergy analyses of the compressor [30].

$$\dot{E}_{cmp} = \dot{m}_r(h_{13} - h_{12}) \tag{20}$$

$$\dot{E}_{cmp,el} = \frac{\dot{E}_{cmp}}{\eta_{is}\,\eta_{mec}} \tag{21}$$

$$\dot{X}_{cmp} = \dot{E}_{cmp,el} + \dot{m}_r(\psi_{12} - \psi_{13}) \tag{22}$$

The following equations can be utilized for the energy and exergy analyses of the expansion valve [30].

$$h_{14} = h_{15} \tag{23}$$

$$\dot{X}_{ev} = \dot{m}_r(\psi_{14} - \psi_{15}) \tag{24}$$

4.4. Fan model

In this study, the dry-bulb temperature of the air inside the building has been set to a constant value of $T_5 = 26$ °C, and the air supply rate to the building ($\dot{m}_{p,a}$) has been determined from Eq. (25). Subsequently, the humidity ratio inside the building (ω_6) has been calculated using Eq. (26) [8]. The airflow in the system varies depending on the building cooling load. The energy and exergy equations for the fans used for the

process and regeneration air were calculated using [16]:

$$\dot{E}_{c,s} = \dot{m}_{p,a} c_{p_{p,a}} (T_6 - T_5) \quad (25)$$

$$\dot{E}_{c,l} = \dot{m}_{p,a} \lambda_{l-v} (\omega_6 - \omega_5) \quad (26)$$

$$\dot{E}_{c,t} = \dot{m}_{p,a} (h_6 - h_5) \quad (27)$$

$$\dot{E}_{fan-1} = \frac{\Delta P_{fan-1} \dot{V}_{p,a}}{\eta_{fan}} \quad (28)$$

$$\dot{E}_{fan-2} = \frac{\Delta P_{fan-2} \dot{V}_{r,a}}{\eta_{fan}} \quad (29)$$

$$\dot{X}_{fan-1} = \dot{E}_{fan-1} + \dot{m}_{p,a} (\psi_4 - \psi_5) \quad (30)$$

$$\dot{X}_{fan-2} = \dot{E}_{fan-2} + \dot{m}_{r,a} (\psi_{10} - \psi_{11}) \quad (31)$$

where, fan-1 and fan-2, respectively, represent the fans in the process and regeneration air ducts and the fan efficiency (η_{fan}), in either case, is assumed to be 0.8.

4.5. Performance parameters

In the study, both energetic and exergetic performance parameters have been considered to determine how much the system improves based on the use of different refrigerants. From an energetic perspective, the performance coefficients of the vapor compression system (COP_r) and the thermal and electrical performance coefficients of the hybrid system (COP_{th} and COP_{el}) have been taken into account [9,37,38].

$$COP_r = \frac{\dot{E}_e}{\dot{E}_{cmp,el}} \quad (32)$$

$$COP_{th} = \frac{\dot{E}_{c,t}}{\dot{E}_{RAH}} \quad (33)$$

$$COP_{el} = \frac{\dot{E}_{c,t}}{\dot{E}_{cms}} \quad (34)$$

$$\dot{E}_{csm} = \dot{E}_{cmp,el} + \dot{E}_{fan-1} + \dot{E}_{fan-2} \quad (35)$$

$$\dot{E}_{RAH} = \dot{E}_{cnd} \quad (36)$$

When evaluated from an exergetic perspective, besides the thermal and electrical performance coefficients ($COP_{x,th}$ and $COP_{x,el}$), the exergy efficiency (η_x) was also taken into account [9].

$$COP_{x,th} = \frac{\dot{X}_{c,t}}{\dot{X}_{reg}} \quad (37)$$

Table 2
Some thermophysical properties of refrigerants [40,41].

Refrigerant	Chemical name	Latent heat of vaporization (kJ/kg) 10 °C	Critical pressure (kPa)	Critical temperature (°C)
R32	Difluoromethane	344	5782	78.4
R1234yf	2,3,3,3-tetrafluoro-1-propene	175.2	3382.2	94.7
R290	Propane	400.8	4251.2	96.67
R134a	Tetrafluoroethane	212.9	4059.3	101.1
R600a	Isobutane	373.4	3629	134.67
R245fa	1,1,1,3,3-Pentafluoropropane	215.1	3651	154.01
R717	Ammonia	1329	11333	132.25

Table 3
Parameters used in the simulation.

Parameter	Value
$T_{i,set}$	26 °C
N_{DW}	12 rev/h
ε_{RHX}	0.85
ΔT_{sh}	3 °C
ΔT_{sc}	3 °C
η_{is}	0.80

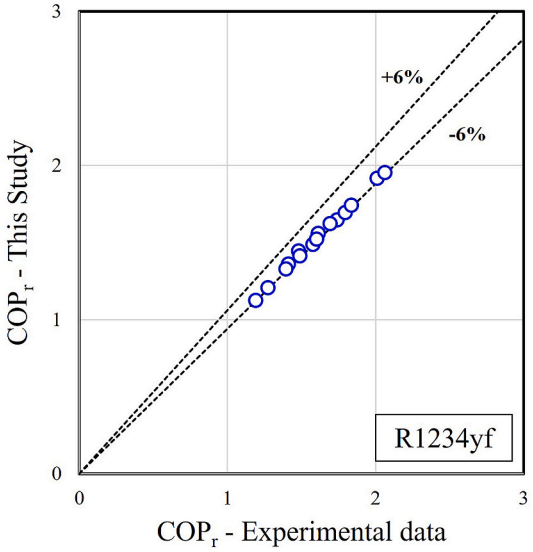

Fig. 5. Comparison of the experimental study [42] obtained from the literature and the results obtained in this study for COP_r.

$$COP_{x,el} = \frac{\dot{X}_{c,t}}{\dot{E}_{csm}} \quad (38)$$

$$\eta_x = 1 - \frac{\dot{X}_{d,t}}{\dot{E}_{csm}} \quad (39)$$

$$\dot{X}_{c,t} = \dot{E}_{c,t} \left[1 - \frac{T_0}{T_{c,avg}} \right] \quad (40)$$

$$\dot{X}_{reg} = \dot{E}_{RAH} \left[1 - \frac{T_0}{T_{reg,avg}} \right] \quad (41)$$

$$\dot{X}_{d,t} = \dot{X}_{cnd} + \dot{X}_e + \dot{X}_{cmp} + \dot{X}_{ev} + \dot{X}_{DW} + \dot{X}_{RHX} + \dot{X}_{fan-1} + \dot{X}_{fan-2} \quad (42)$$

where, the total exergy destruction rate ($\dot{X}_{d,t}$) is obtained by summing up the exergy destruction rates obtained for each equipment.

5. Results and discussion

In this study, energetic and exergetic analyses of the integrated DW-VC cooling system for an office were conducted based on the use of different refrigerants. The refrigerants used were R32, R1234yf, R290, R134a, R600a, R245fa, and R717, respectively. These refrigerants share the common characteristic of having zero Ozone Depletion Potential (ODP). Some thermophysical properties of the available refrigerants are presented in Table 2. To perform the energetic and exergetic analyses of the DW-VC cooling system, simultaneous solution of multiple equations is required, as discussed in the previous section. This involves an iterative approach for certain variables. Additionally, relationships between thermophysical properties of moist air and refrigerants are needed for

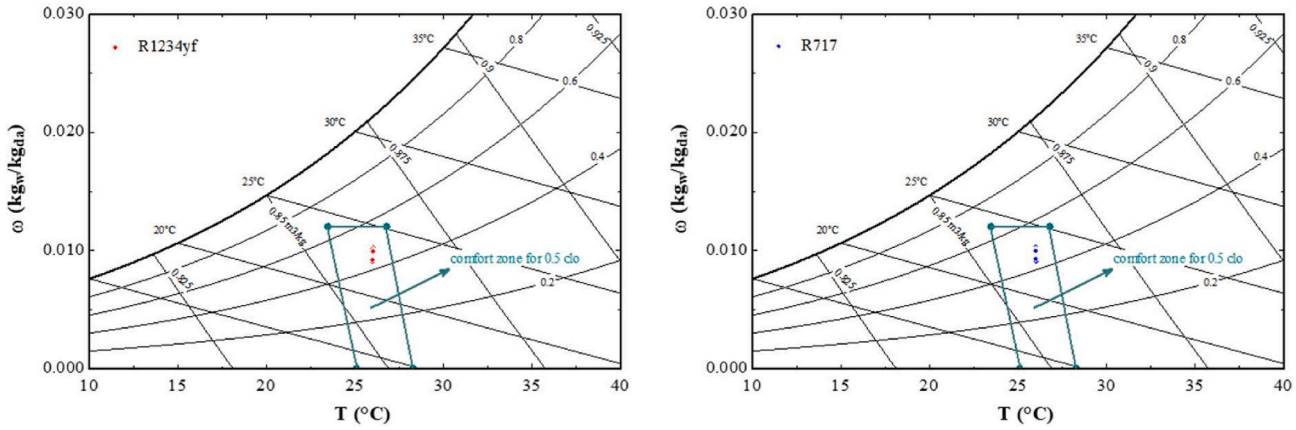

Fig. 6. Comfort zone and indoor air properties for R1234yf and R717 refrigerants.

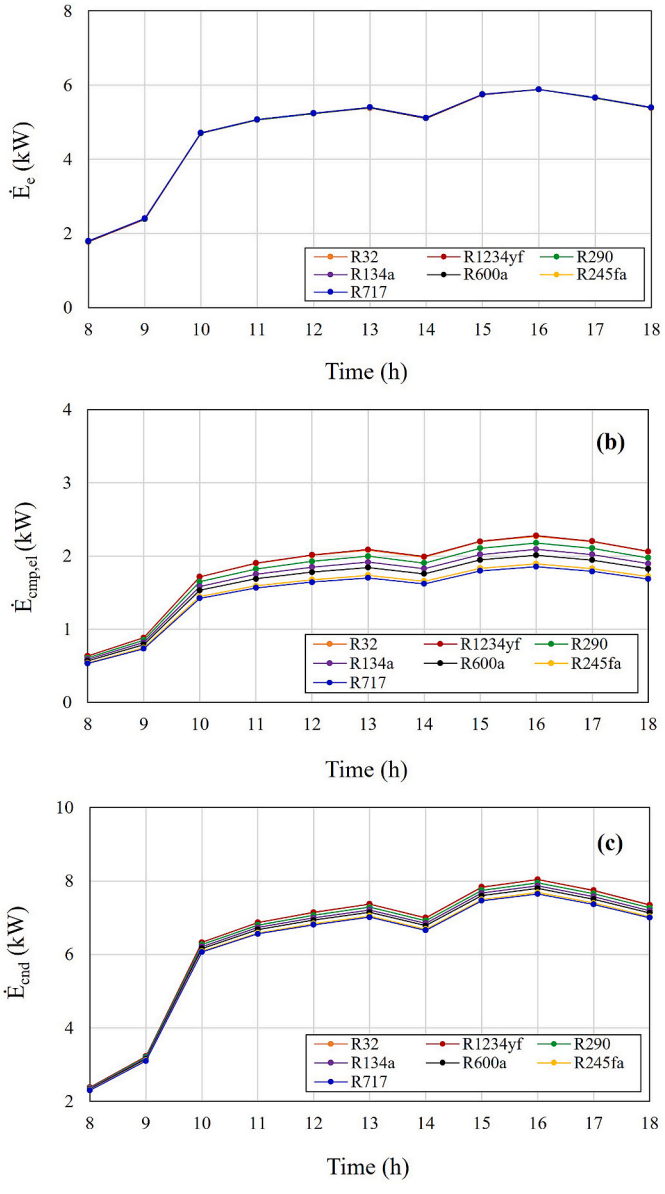

Fig. 7. Variations in evaporator capacity-$\dot{E}_e$ (a), compressor power consumption-$\dot{E}_{cmp,el}$ (b), and condenser capacity-$\dot{E}_{cnd}$ (c) during office working hours.

the solution. Therefore, the defined mathematical equations were solved using the Engineering Equation Solver (EES) software [39]. Climate data for a year of Istanbul, specifically for the 23rd day of the highest cooling load in August, were used for this case study. Simulations were conducted considering the system parameters in Table 3.

5.1. Validation of vapor compression system

The assumptions used for the traditional vapor compression system in the study are widely employed in the literature. Additionally, in this study, experimental COP_r data obtained for a refrigerant (R1234yf) from the work conducted by Sieres and Santos [42] were used for validation (Fig. 5). Since no specific details were provided regarding the isentropic efficiency of the compressor, the overall efficiency of the compressor was determined considering the ratio of isentropic power to electrical power. All values were found to be below ±6 % relative error, with a maximum relative error of 5.65 %. Upon observing Fig. 5, it is evident that the obtained results align well with the literature, indicating the appropriateness of the assumptions used for the vapor compression system.

5.2. Energetic comparison of the hybrid DW-VC cooling system

The comfort zone defined by ASHRAE Standard 55 [43] and the indoor conditions provided by the system for R1234yf and R717 refrigerants are presented on the psychrometric chart (Fig. 6). From the figure, it is observed that the indoor conditions are nearly identical for both refrigerants. This results in the conclusion that indoor comfort conditions are maintained with the use of all refrigerants throughout office working hours.

As expected, the capacity of the evaporator, the last components of process channel, exhibited a trend similar to the total cooling load throughout the day to meet the desired indoor comfort conditions, and almost identical capacity values were obtained for all refrigerants (Fig. 7-a). Additionally, some condensation occurred as the evaporator surface temperature was below the dew point temperature of the process air (Fig. 8).

With compressor electricity consumption, the highest power consumption was observed in the VCS using R1234yf refrigerant (Fig. 7-b and 8). In the VCS using R32, which had the second-highest power consumption, the obtained electrical consumption value was nearly the same as that of R1234yf. The main reasons for this high consumption are the low latent heat of evaporation of R1234yf and the low critical temperature of R32. Since the evaporation latent heat of R717 is the highest, in the system where this refrigerant is used, better heat transfer occurred during the evaporation process compared to other refrigerants. As a result, the system using R717 achieved the lowest compressor

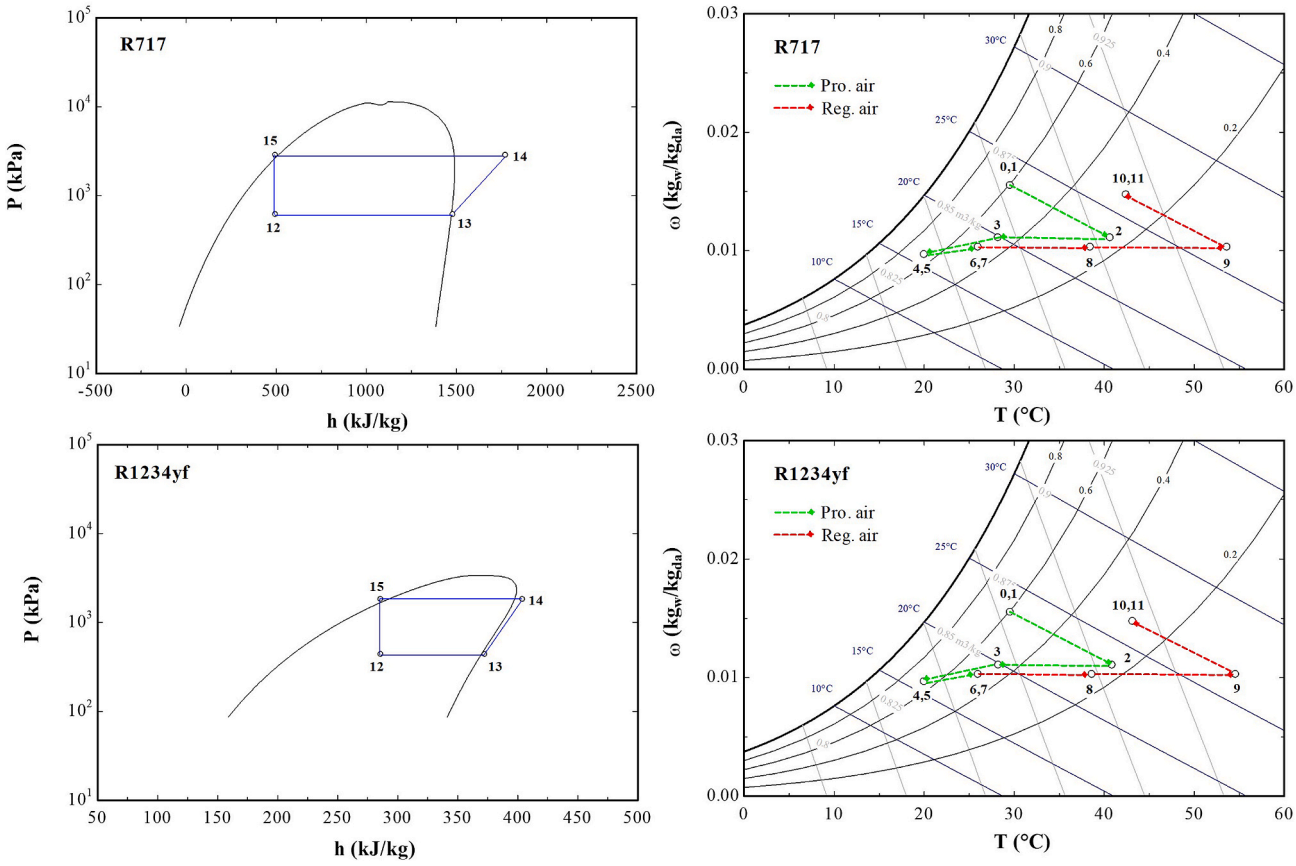

Fig. 8. Variations in the P-h and psychrometric charts at 15:00 for the use of R717 and R1234yf refrigerants.

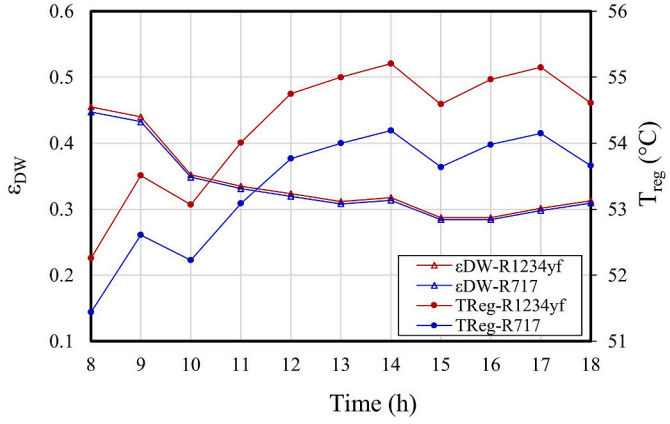

Fig. 9. Variations in ε_{DW} and T_{reg} during office working hours.

electricity consumption (Fig. 7-b and Fig. 8). The second-lowest compressor electrical consumption corresponds to the system using R245fa, which has the highest critical temperature. Compared to R1234yf, the power consumption of compressors in R717 and R245fa decreased by 18.2 % and 16.6 %, respectively.

From the use of R717 to the use of R1234yf, an increase in compressor power consumption was accompanied by an increase in condenser capacity (Fig. 7-c). However, this increase was not as pronounced as that with the compressor.

The higher compressor power consumption results in a higher heat rate being rejected from the condenser to the regeneration air. Since the heat rejected from the condenser is also utilized as the regeneration heat of the desiccant wheel, the highest regeneration heat was obtained with

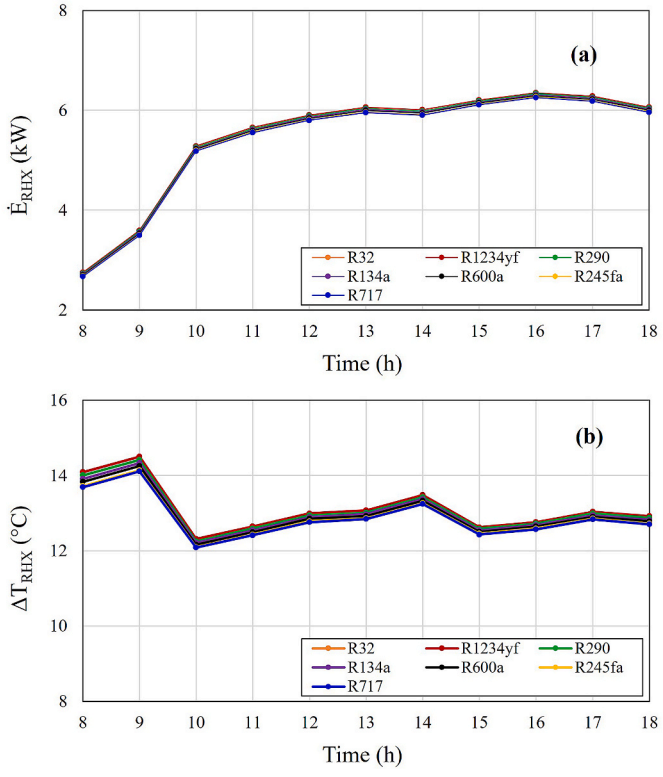

Fig. 10. Variations in heat transfer rate ($\dot{E}_{RHX}$) and temperature difference (ΔT_{RHX}) in RHX during office working hours.

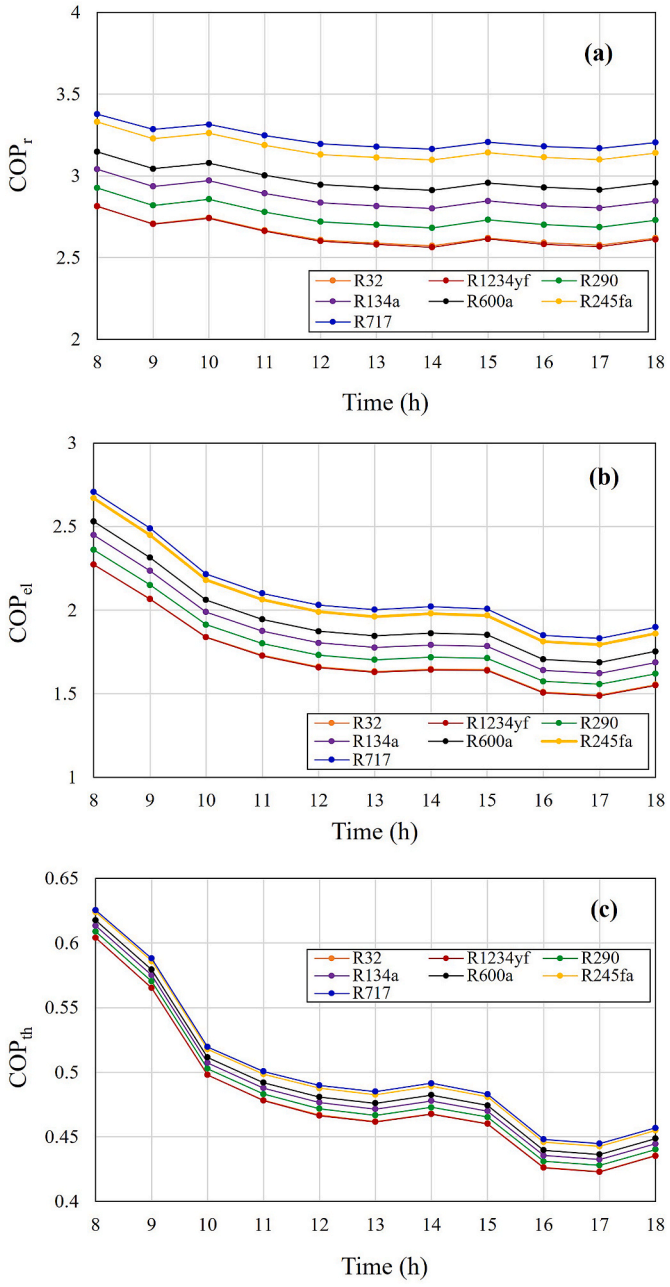

Fig. 11. Variations in COP_r (a), COP_{el}, (b) and COP_{th} (c) during office working hours.

R1234yf, and the lowest regeneration heat was obtained with R717 (Fig. 7-c). Due to the higher regeneration heat obtained compared to others in R1234yf, higher regeneration temperatures were achieved with R1234yf. The higher regeneration temperature increases the amount of moisture extracted from the process air by the desiccant wheel, thereby improving the dehumidification effectiveness (ε_{DW}) of the desiccant wheel. This resulted in the highest ε_{DW} in the system using R1234yf and the lowest ε_{DW} values in the system using R717 (Fig. 9). A 1.33 % increase in ε_{DW} was obtained in the system using R1234yf compared with the system using R717. Additionally, despite the increase in regeneration heat with the increase in cooling load, ε_{DW} decreased for all cases. This is because the increase in regeneration temperature is proportionally less than the increase in cooling load.

Thanks to the sensible heat transfer that occurs in the Rotating Heat Exchanger (RHX), it is observed that, on one hand, the cooling load of the evaporator is reduced, and on the other hand, required regeneration

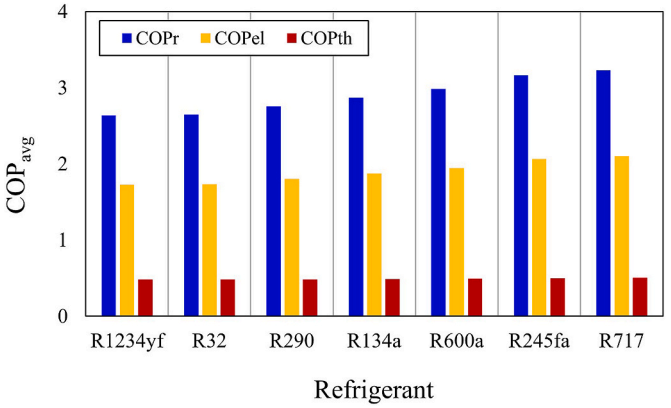

Fig. 12. Variations in the daily average energetic performance parameters of the system.

temperatures can be reached without the need for an additional heater (Fig. 10-a). For the cases where R1234yf and R717 refrigerants were used, the temperature differences during office working hours varied in the ranges of 12.25–14.5 °C and 12.08–14.11 °C, respectively (Fig. 10-b). The slight differences in these ranges are due to the temperature and absolute humidity of the air exiting the DW.

When examining the variation of the system energetic performance parameters during office working hours, it is observed that all performance parameters exhibit a reverse trend to the cooling load (Fig. 11). As seen in Fig. 12, the highest variation during working hours is observed for COP_{el}, while relatively less variation is determined for COP_r and COP_{th}. Looking at the daily average variations of the performance parameters, the highest values are obtained for R717 (COP_r = 3.23, COP_{el} = 2.11 and COP_{th} = 0.51), the second-highest for R245fa, the lowest for R1234yf (COP_r = 2.64, COP_{el} = 1.73 and COP_{th} = 0.48), and the second-lowest for R32. Compared to R1234yf, the increase in COP_r, COP_{el}, and COP_{th} parameters in R717 is 22.3 %, 21.8 %, and 4.7 %, respectively. Similarly, compared to R1234yf, the increase in COP_r, COP_{el}, and COP_{th} parameters in R245fa is 20.0 %, 19.5 %, and 4.3 %, respectively. Considering the energetic performance parameters, it is observed that the refrigerant most suitable for the current system is R717.

5.3. Exergetic comparison of the hybrid DW-VC cooling system

In Fig. 13-a, the exergy variation ($\dot{X}_{c,t}$) of the building cooling load during working hours is provided. Since this parameter changes depending on the cooling load, supply temperature (T_5), and indoor temperature (T_6), it is not influenced by the refrigerants. $\dot{X}_{reg}$, $\dot{E}_{csm}$, and $\dot{X}_{d,t}$ are shown similar trends throughout the day, reaching their highest values at the time (16:00) when the sensible heat load is the highest (Fig. 13-b, c, d). As can be understood from the figure, systems using refrigerants with the lowest electrical consumption also have the lowest exergy destruction. Compared to the system using R1234yf, the average electrical consumption ($\dot{E}_{csm}$) and exergy destruction ($\dot{X}_{d,t}$) in the system using R717 decreased by 13.10 % and 13.78 %, respectively.

When examining the daily variation of performance parameters for desiccant cooling systems using all refrigerants, the $COP_{x,el}$ parameter reaches its highest value at 14:00, while the $COP_{x,th}$ and η_x parameters reach their highest values at 15:00 (Fig. 14). At 14:00, a decrease in electricity consumption similar to the decrease in cooling load resulted in achieving the highest values of $COP_{x,el}$ (Figs. 7 and 13). Similar to the energetic analysis results, as seen in Fig. 15 the highest daily average performance parameters are obtained for R717 ($COP_{x,el}$ = 0.022, $COP_{x,th}$ = 0.1411 and η_x = 8.40 %) while the lowest daily average performance values are obtained for R1234yf ($COP_{x,el}$ = 0.019, $COP_{x,th}$ = 0.1303 and η_x = 7.71 %). The second-highest daily average performance

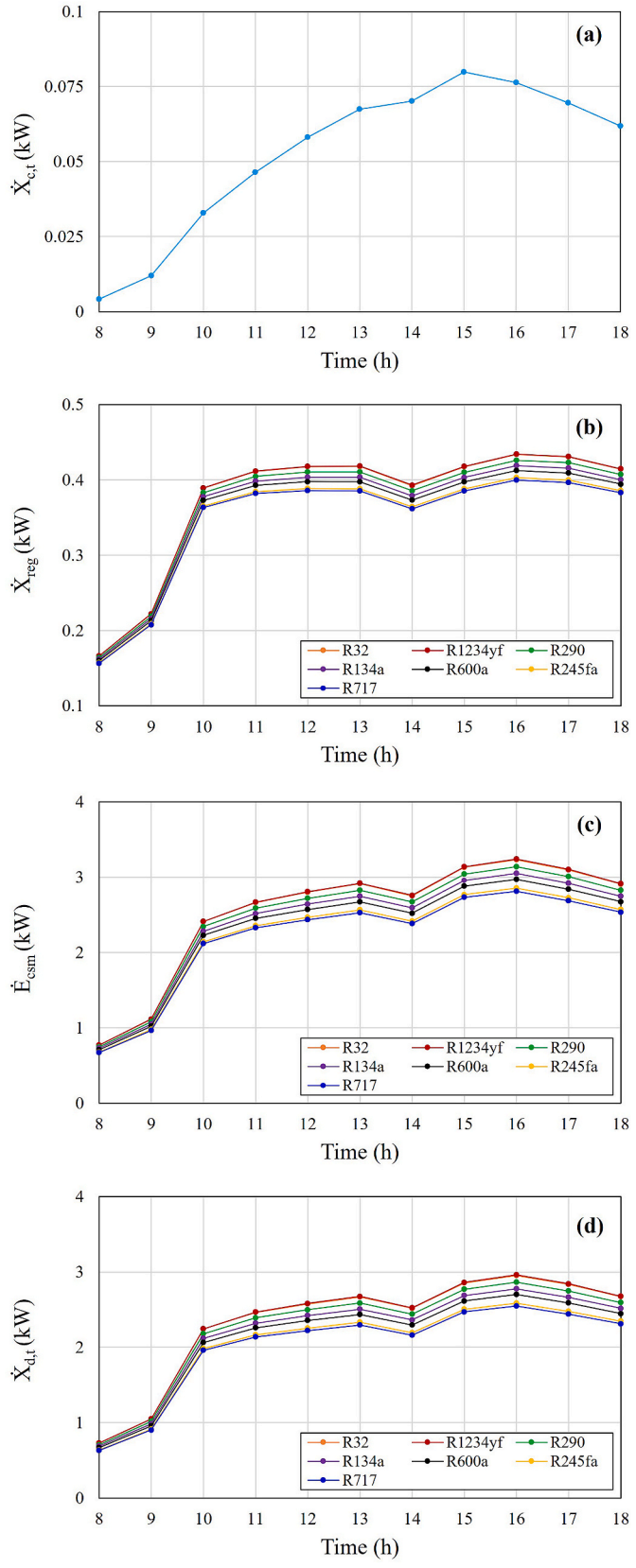

Fig. 13. Variations in $\dot{X}_{c,t}$ (a), $\dot{X}_{reg}$ (b), $\dot{E}_{cms}$, (c) and $\dot{X}_{d,t}$ (d) during office working hours.

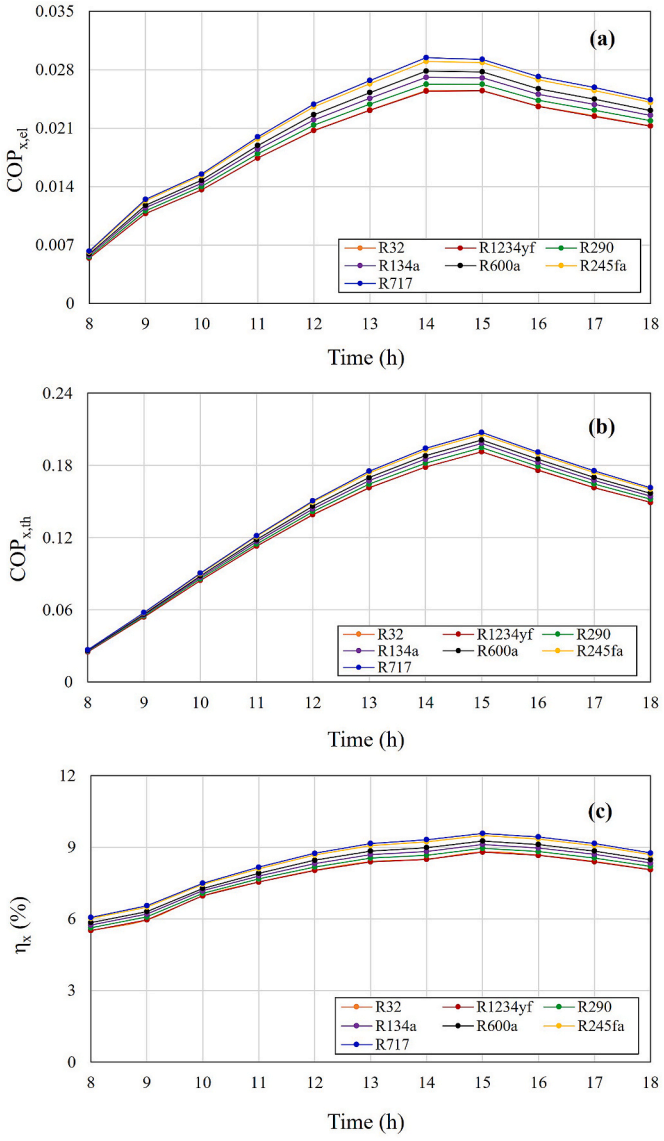

Fig. 14. Variations in $COP_{x,el}$ (a), $COP_{x,th}$, (b) and η_x (c) during office working hours.

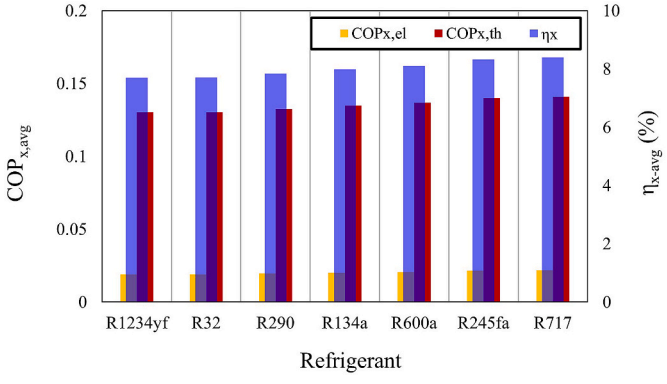

Fig. 15. Variations in the daily average exergetic performance parameters of the system.

parameters are found for R245fa. Compared to R1234yf, the $COP_{x,el}$, $COP_{x,th}$, and η_x of R717 increased by 15.2 %, 8.3 %, and 9.0 %, respectively. The use of R717 in the system resulted in reductions in exergy destruction compared to the use of R1234yf. This significantly improved the exergy performance parameters ($COP_{x,el}$ and $COP_{x,th}$) and the exergy efficiency (η_x) of the system. For R245fa, the $COP_{x,el}$, $COP_{x,th}$ and η_x increased by 13.6 %, 7.5 %, and 8.1 %, respectively. The exergetic performance parameters obtained for R32 are almost the same as those for R1234yf.

In general, the highest energy and exergy performance parameters in the system were achieved with the use of R717 as refrigerant. This will reduce energy consumption and thus provide energy savings through the use of R717 refrigerant in the current system. The decrease in energy consumption in the system also offer significant potential contributions, especially to cooling systems that will be used in nearly zero-energy buildings.

In the literature, it is mentioned that harmful refrigerants chemically break down ozone into oxygen, leading to increased global warming due to harmful UV radiation entering the Earth's surface. Therefore, it is necessary to use refrigerants in the system with zero ODP and a GWP of less than 150 [44]. In addition to having the highest energetic and exergetic performance parameters, another advantage of R717 ($GWP_{R717} = 0$) over R245fa ($GWP_{R245fa} = 1050$), which has the second-highest performance parameters, is its much lower Global Warming Potential (GWP) [41]. This works further in favor of using R717 in current desiccant cooling systems. The difference in energetic and exergetic performance parameters between R1234yf and R32, which have the lowest energetic and exergetic performance parameters, is almost negligible. At the same time, the GWP of R1234yf ($GWP_{R1234yf} < 1$) is much lower than that of R32 ($GWP_{R32} = 675$) [38,44]. In the literature, R1234yf was recognized as one of the refrigerants of the 21st century due to its low flammability and environmentally friendly properties (zero ODP and low GWP) [44]. These may be the reasons for preferring R1234yf over R32 in current desiccant cooling systems. Furthermore, it was observed that R600a generally outperforms R134a and R32, which is restricted in its use, in terms of both energetic and exergetic performance.

6. Conclusions

In this study, the variation in energetic and exergetic performance parameters of a hybrid rotary desiccant – vapor compression refrigeration system was investigated based on the use of different refrigerants. Hourly simulations of the hybrid cooling system were conducted for a 100 m^2 office building located in Istanbul, Turkey. The main conclusions are as follows.

- All refrigerants provided indoor office comfort conditions, as defined by ASHRAE Standard 55, under the cooling conditions defined in this paper.
- The highest electrical power consumption was found to be the highest when R1234yf was used as the refrigerant, followed by R32 with a similar value. The lowest electrical power consumption was found with R717 followed by R245fa. Comparing the power consumption of R1234yf with R717 and R245fa, the compressor power consumption decreased by 18.2 % and 16.6 %, respectively.
- R1234yf has the highest heat regeneration which positively affects the desiccant wheel effectiveness, and R717 has the lowest value. However, when both refrigerants are compared, the effect on desiccant wheel effectiveness is not significant with an increase of 1.33 %.
- The highest energetic performance parameters were obtained for R717, while the lowest energetic performance parameters were obtained for R1234yf. Compared to R1234yf, the increase in daily average COP_r, COP_{el}, and COP_{th} parameters in R717 is 22.3 %, 21.8 %, and 4.7 %, respectively.
- The lowest total exergy destruction rate and regeneration exergy rate were observed in R717, which also had the lowest electricity consumption. The highest values were obtained from the results for R1234yf.
- In the daily average exergy performance parameters as well, the highest results were obtained in R717, which has the lowest exergy destruction. Compared to R1234yf, which had the lowest results, daily average $COP_{x,el}$, $COP_{x,th}$, and η_x increased by 13.6 %, 7.5 %, and 8.1 %, respectively, in R717.

The results obtained in the study favor the use of R717 in hybrid DW-VC cooling systems due to superior energetic and exergetic performance parameters compared with those of the other refrigerants studied here. Another refrigerant with low Global Warming Potential (GWP), R600a, enhances the system performance compared to R134a and R32. R1234yf, which has almost the same performance parameters as R32, becomes more attractive due to its lower GWP compared with that of R32.

CRediT authorship contribution statement

Kamil Neyfel Çerçi: Writing – original draft, Methodology, Investigation, Conceptualization, Writing – review & editing. **Ivo Rafael Oliveira Silva:** Validation, Investigation, Visualization. **Kamel Hooman:** Writing – review & editing, Resources.

Declaration of competing interest

The authors declare that they have no known competing financial interests or personal relationships that could have appeared to influence the work reported in this paper.

Data availability

The authors are unable or have chosen not to specify which data has been used.

Acknowledgement

We would like to thank the Scientific and Technological Research Council of Türkiye (TUBITAK), International Postdoctoral Research Fellowship Program (TUBITAK 2219) for financially supporting (Grant number:1059B192203025) Dr. Kamil Neyfel Çerçi.

Appendix A

See Table A.1.

Table A.1
Coefficients of MLR model for T_2 and ω_2 [28]

Estimates	x_i	$T_{p,o}$ [°C]	$\omega_{p,o}$ [g kg^{-1}]
c_0	–	−10.64513	4.147455
c_1	N_{DW}	−0.7319	0.171803
c_2	V_{DW}	3.022259	−1.569075
c_3	T_1	0.519742	0.099211
c_4	ω_1	1.394057	0.2786
c_5	T_9	0.68969	−0.161955
c_6	ω_9	−0.54944	0.378153
c_7	N_{DW}•N_{DW}	0.005699	–
c_8	N_{DW}•T_1	0.004843	−0.003639
c_9	N_{DW}•T_9	0.009573	−0.001563
c_{10}	V_{DW}•V_{DW}	–	0.071792
c_{11}	V_{DW}•ω_1	0.032986	0.041421
c_{12}	V_{DW}•T_9	−0.08979	0.021829
c_{13}	V_{DW}•ω_9	–	−0.034065
c_{14}	T_1•T_9	0.002027	–
c_{15}	T_1•ω_1	−0.012673	0.005935
c_{16}	ω_1•ω_1	−0.018022	–
c_{17}	ω_1•T_9	0.011085	−0.003591
c_{18}	ω_1•ω_9	−0.04198	0.016637
c_{19}	T_9•T_9	−0.002995	0.000801
c_{20}	T_9•ω_9	–	−0.001611
c_{21}	ω_9•ω_9	0.029884	−0.006499

References

[1] Omer AM. Energy, environment and sustainable development. Renew Sustain Energy Rev 2008;12:2265–300. https://doi.org/10.1016/j.rser.2007.05.001.
[2] Yang L, Yan H, Lam JC. Thermal comfort and building energy consumption implications – a review. Appl Energy 2014;115:164–73. https://doi.org/10.1016/j.apenergy.2013.10.062.
[3] Comino F, Ruiz de Adana M, Peci F. Energy saving potential of a hybrid HVAC system with a desiccant wheel activated at low temperatures and an indirect evaporative cooler in handling air in buildings with high latent loads. Appl Therm Eng 2018;131:412–27. https://doi.org/10.1016/j.applthermaleng.2017.12.004.
[4] Niu JL, Zhang LZ, Zuo HG. Energy savings potential of chilled-ceiling combined with desiccant cooling in hot and humid climates. Energy Build 2002;34:487–95. https://doi.org/10.1016/S0378-7788(01)00132-3.
[5] Uçkan İ, Yılmaz T, Hürdoğan E, Büyükalaca O. Development of an artificial neural network model for the prediction of the performance of a silica-gel desiccant wheel. Int J Green Energy 2015;12:1159–68. https://doi.org/10.1080/15435075.2014.895733.
[6] Tian S, Su X, Geng Y, Li H, Liang Y, Di Y. Heat pump combined with single-stage or two-stage desiccant wheel system? A comparative study on different humidity requirement buildings. Energy Convers Manag 2022;255:115345. https://doi.org/10.1016/j.enconman.2022.115345.
[7] Ge TS, Ziegler F, Wang RZ, Wang H. Performance comparison between a solar driven rotary desiccant cooling system and conventional vapor compression system (performance study of desiccant cooling). Appl Therm Eng 2010;30:724–31. https://doi.org/10.1016/j.applthermaleng.2009.12.002.
[8] Olmuş U, Güzelel YE, Büyükalaca O. Seasonal analysis of a desiccant air-conditioning system supported by water-cooled PV/T units. Energy Build 2023;291:113101. https://doi.org/10.1016/j.enbuild.2023.113101.
[9] Caliskan H, Lee D-Y, Hong H. Enhanced thermodynamic assessments of the novel desiccant air cooling system for sustainable energy future. J Clean Prod 2019;211:213–21. https://doi.org/10.1016/j.jclepro.2018.11.174.
[10] Hwang W-B, Choi S, Lee D-Y. In-depth analysis of the performance of hybrid desiccant cooling system incorporated with an electric heat pump. Energy 2017;118:324–32. https://doi.org/10.1016/j.energy.2016.12.007.
[11] Tian S, Su X, Li H, Huang Y. Using a coupled heat pump desiccant wheel system to improve indoor humidity environment of nZEB in Shanghai: Analysis and optimization. Build Environ 2021;206:108391. https://doi.org/10.1016/j.buildenv.2021.108391.
[12] Tian S, Su X, Shao X, Wang L. Optimization and evaluation of a solar energy, heat pump and desiccant wheel hybrid system in a nearly zero energy building. Build Simul 2020;13:1291–303. https://doi.org/10.1007/s12273-020-0627-0.
[13] Ge F, Wang C. Exergy analysis of dehumidification systems: a comparison between the condensing dehumidification and the desiccant wheel dehumidification. Energy Convers Manag 2020;224:113343. https://doi.org/10.1016/j.enconman.2020.113343.
[14] Ge F, Guo X, Hu Z, Chu Y. Energy savings potential of a desiccant assisted hybrid air source heat pump system for residential building in hot summer and cold winter zone in China. Energy Build 2011;43:3521–7. https://doi.org/10.1016/j.enbuild.2011.09.021.
[15] Liu W, Lian Z, Radermacher R, Yao Y. Energy consumption analysis on a dedicated outdoor air system with rotary desiccant wheel. Energy 2007;32:1749–60. https://doi.org/10.1016/j.energy.2006.11.012.
[16] Hürdoğan E, Buyükalaca O, Hepbasli A, Yılmaz T. Exergetic modeling and experimental performance assessment of a novel desiccant cooling system. Energy Build 2011;43:1489–98. https://doi.org/10.1016/j.enbuild.2011.02.016.
[17] Jani DB, Mishra M, Sahoo PK. Performance studies of hybrid solid desiccant–vapor compression air-conditioning system for hot and humid climates. Energy Build 2015;102:284–92. https://doi.org/10.1016/j.enbuild.2015.05.055.
[18] Jani DB, Mishra M, Sahoo PK. Performance analysis of a solid desiccant assisted hybrid space cooling system using TRNSYS. J Build Eng 2018;19:26–35. https://doi.org/10.1016/j.jobe.2018.04.016.
[19] Tu R, Liu X-H, Jiang Y. Irreversible processes and performance improvement of desiccant wheel dehumidification and cooling systems using exergy. Appl Energy 2015;145:331–44. https://doi.org/10.1016/j.apenergy.2015.02.043.
[20] Sheng Y, Zhang Y, Deng N, Fang L, Nie J, Ma L. Experimental analysis on performance of high temperature heat pump and desiccant wheel system. Energy Build 2013;66:505–13. https://doi.org/10.1016/j.enbuild.2013.07.058.
[21] Sheng Y, Zhang Y, Sun Y, Ding G. Thermodynamic analysis of desiccant wheel coupled to high-temperature heat pump system. Sci Technol Built Environ 2015;21:1165–74. https://doi.org/10.1080/23744731.2015.1056656.
[22] Lo Basso G, de Santoli L, Paiolo R, Losi C. The potential role of trans-critical CO2 heat pumps within a solar cooling system for building services: the hybridised system energy analysis by a dynamic simulation model. Renew Energy 2021;164:472–90. https://doi.org/10.1016/j.renene.2020.09.098.
[23] Regulation (EU. No 517/2014 of the European Parliament and the Council of 16 April 2014 on fluorinated greenhouse gases and repealing regulation (EC) No 842/2006. Off J Eur Union 2014;150:195–230 [n.d.].
[24] Klein, S.A. TRNSYS 18: A Transient System Simulation Program. Solar Energy Laboratory; The University of Wisconsin: Madison, WI, USA, 2017; Volume 3.
[25] TS. Thermal insulation in buildings. Ankara: Official gazette; 2013. n.d.
[26] Goel S, Rosenberg MI, Eley C. ANSI/ASHRAE/IES standard 90.1-2016 performance rating method reference manual. 2017. https://doi.org/10.2172/1398228. Richland, WA (United States).
[27] Crawley DB, Lawrie LK, Army US, Champaign C, Curtis I, Pedersen O, Winkelmann FC. EnergyPlus: energy simulation program, ASHRAE J 2000;42:49–56. 10.1.1.122.6852.
[28] Güzelel YE, Olmuş U, Çerçi KN, Büyükalaca O. Comprehensive modelling of rotary desiccant wheel with different multiple regression and machine learning methods for balanced flow. Appl Therm Eng 2021;199:117544. https://doi.org/10.1016/j.applthermaleng.2021.117544.
[29] Olmuş U, Güzelel YE, Pınar E, Özbek A, Büyükalaca O. Performance assessment of a desiccant air-conditioning system combined with dew-point indirect evaporative cooler and PV/T. Sol Energy 2022;231:566–77. https://doi.org/10.1016/j.solener.2021.12.004.
[30] Mete Ozturk M, Doğan B, Berrin Erbay L. Performance assessment of an air source heat pump water heater from exergy aspect. Sustain Energy Technol Assessments 2020;42:100809. https://doi.org/10.1016/j.seta.2020.100809.
[31] Kanoğlu M, Özdinç Çarpınlıoğlu M, Yıldırım M. Energy and exergy analyses of an experimental open-cycle desiccant cooling system. Appl Therm Eng 2004;24:919–32. https://doi.org/10.1016/j.applthermaleng.2003.10.003.
[32] Kays WM, London A. Compact heat exchangers. third ed. McGraw-Hill; 1984.

[33] Song J, Sobhani B. Energy and exergy performance of an integrated desiccant cooling system with photovoltaic/thermal using phase change material and maisotsenko cooler. J Energy Storage 2020;32:101698. https://doi.org/10.1016/j.est.2020.101698.
[34] Kutlu C, Erdinc MT, Li J, Wang Y, Su Y. A study on heat storage sizing and flow control for a domestic scale solar-powered organic Rankine cycle-vapour compression refrigeration system. Renew Energy 2019;143:301–12. https://doi.org/10.1016/j.renene.2019.05.017.
[35] Erdinc MT. Two-evaporator refrigeration system integrated with expander-compressor booster. Int J Refrig 2023;154:349–63. https://doi.org/10.1016/j.ijrefrig.2023.06.023.
[36] De Antonellis S, Joppolo CM, Molinaroli L, Pasini A. Simulation and energy efficiency analysis of desiccant wheel systems for drying processes. Energy 2012;37:336–45. https://doi.org/10.1016/j.energy.2011.11.021.
[37] Güzelel YE, Olmuş U, Büyükalaca O. Simulation of a desiccant air-conditioning system integrated with dew-point indirect evaporative cooler for a school building. Appl Therm Eng 2022;217:119233. https://doi.org/10.1016/j.applthermaleng.2022.119233.
[38] Yilmaz T, Erdinç MT. Energetic and exergetic investigation of a novel refrigeration system utilizing ejector integrated subcooling using different refrigerants. Energy 2019;168:712–27. https://doi.org/10.1016/j.energy.2018.11.081.
[39] Klein SA. Engineering equation solver academic professional, V10.442. F-Chart Software; 2012.
[40] Ashrae fundemantals handbook. 2013.
[41] Besagni G, Mereu R, Inzoli F. Ejector refrigeration: a comprehensive review. Renew Sustain Energy Rev 2016;53:373–407. https://doi.org/10.1016/j.rser.2015.08.059.
[42] Sieres J, Santos JM. Experimental analysis of R1234yf as a drop-in replacement for R134a in a small power refrigerating system. Int J Refrig 2018;91:230–8. https://doi.org/10.1016/j.ijrefrig.2018.05.019.
[43] ASHRAE-Standard-55. Thermal environmental conditions for human occupancy, American society of heating refrigerating, and air-conditioning engineers. 2017.
[44] Yadav S, Liu J, Kim SC. A comprehensive study on 21st-century refrigerants - R290 and R1234yf: a review. Int J Heat Mass Transf 2022;182. https://doi.org/10.1016/j.ijheatmasstransfer.2021.121947.